

Formation of Gold Nanoparticles by Good's Buffers

Ahsan Habib, Masaaki Tabata,* and Ying Guang Wu

Department of Chemistry, Faculty of Science and Engineering, Saga University, 1, Honjo-machi, Saga 840-8502

Received June 18, 2004; E-mail: tabatam@cc.saga-u.ac.jp

Gold nanoparticle formation was found from tetrachloroaurate(III) in the presence of Good's Buffers, such as 2-morpholinoethanesulfonic acid (MES) and 2-[4-(2-hydroxyethyl)-1-piperazinyl]ethanesulfonic acid (HEPES), which are used widely in laboratories for studies of analytical, inorganic, physical, and bio-chemistry as well as biology. The obtained gold nanoparticles were examined by Ultraviolet–Visible Spectroscopy (UV–vis), Dynamic Light Scattering (DLS) and Electrophoretic Light Scattering (ELS) in an aqueous system and by transmission electron microscopy (TEM) for particle morphologies. UV–vis spectra showed absorption maxima at ~530 and ~750 nm, depending on the buffer reagents and their concentration, pH, and ionic strength. The size and the surface zeta potential of the formed nanoparticles were 23 to 73 nm and −30 to −12 mV, respectively. The TEM pictures clearly indicated the formation of finely dispersed, chained, or aggregated gold nanoparticles, depending on the experimental conditions. The mechanism of gold nanoparticle formation was studied by the measurements of cyclic voltammetry (CV) and electron spin resonance (ESR). MES and HEPES showed a positive anodic peak at approximately +800 mV vs Ag/AgCl electrode, which indicated that these buffering agents have mild reducing ability. ESR results indicated the generation of nitrogen-centered cationic free radicals from these Good's Buffers in the presence of Au(III), resulting in the formation of gold nanoparticles. A reaction mechanism is proposed.

Interest in the preparation and characterization of nanoparticles has grown significantly because of their diversified uses in nanodevices[1] as well as in cell biology as biological sensors.[2–5] It has attracted the avid attention of chemists, physicists, and engineers, who wish to use them for the development of new-generation nanodevices. Studies and applications of gold nanoparticles could be traced back through centuries. During the last few decades, however, interest in gold nanoparticles to chemists, biochemists, and biologists has boomed, since they can be used as effective labeling agents or markers for the precise detection of ultra-structural localization, distribution and quantization of macromolecules in living or fixed cells or tissues.[6,7] The detection of DNA by using gold nanoparticles has also been reported.[8–12]

Good's Buffers are popular pH buffers that are widely used in laboratories of analytical, inorganic, physical, biological, and biochemistry as well as in tissue culturing.[13–16] This is because of their convenient pK_a values of between 6 and 8, maximum aqueous solubility with minimum solubility in other solvents, low ability to cross biological membranes, minimal effects due to ionic composition, concentration or temperature, high chemical stability, and supposedly low affinities for metal ions, which are usually used in many biological systems.[13,14] Of the Good's Buffers developed to date, 2-[4-(2-hydroxyethyl)-1-piperazinyl]ethanesulfonic acid (HEPES, pK_a = 7.55) has been used in different fields ranging from tissue culture to analytical methods. However, recent studies indicate that Good's Buffers are not inert, as was previously believed. Good's Buffers containing piperazine rings are able to generate nitrogen-centered free radicals in the presence of Fe(II), Fe(III)–polymer, and molecular oxygen.[17,18] HEPES has been shown to reduce Cu(II) to Cu(I) in the presence of ligands that stabilize Cu(I).[19] Moreover, some Good's Buffers have also shown significant affinities to a number of metal ions, resulting in the formation of metal complexes having appreciable association constants.[20–23]

In the present work, we found the formation of gold nanoparticles from Good's Buffers, such as 2-morpholinoethanesulfonic acid (MES, pK_a = 6.15) and 2-[4-(2-hydroxyethyl)-1-piperazinyl]ethanesulfonic acid (HEPES). We have characterized the formation of gold nanoparticles and their size distribution as well as their stability under various experimental conditions. Moreover, we have investigated the reactivities of Good's Buffers in the presence of Au(III). These buffer reagents reduced Au(III) to Au(II)/Au(I), and finally to Au(0), resulting in the formation of gold nanoparticles. ESR data have indicated the formation of nitrogen-centered cationic free radicals from the Good's Buffers in the presence of Au(III) during redox reactions. Moreover, the present study could provide information about the toxicities of Good's Buffers in vitro studies where Au(III) is involved.[24]

Experimental

Reagents. Good's Buffers, including HEPES, MES, 3-morpholinopropanesulfonic acid (MOPS, pK_a = 7.20), 2-hydroxy-3-morpholinopropanesulfonic acid (MOPSO, pK_a = 6.95), 3-[4-(2-hydroxyethyl)-1-piperazinyl]propanesulfonic acid (EPPS, pK_a = 8.0), 2-hydroxy-3-[4-(2-hydroxyethyl)-1-piperazinyl]propanesulfonic acid (HEPPSO, pK_a = 7.90), and piperazine-1,4-bis(2-ethanesulfonic acid) (PIPES, pK_a = 6.80), were purchased from Dojindo Laboratories Ltd., Japan. Sodium tetrachloroaurate(III) dihydrate, sodium chloride, sodium sulfate, and sodium hydroxide were purchased from Wako Pure Chemical Industries Ltd., Japan. *N-tert*-butyl-α-phenylnitrone (PBN) was purchased from Aldrich

Published on the web February 11, 2005; DOI 10.1246/bcsj.78.262

Chem. Co., Japan. A stock solution of Au(III) of 3.00×10^{-3} mol dm^{-3} was prepared by dissolving $NaAuCl_4 \cdot 2H_2O$ in doubly distilled water, and kept in the dark. The Au(III) concentration of the stock solution was determined by atomic absorption spectroscopy (AAS). Aqueous solutions of HEPES and MES were prepared by dissolution of the respective standard Good's Buffers solutions. Doubly deionized water was used throughout the experiments.

Apparatus. UV–visible absorption spectra were recorded on a JASCO spectrophotometer (Model V-550, Japan) at 25 °C with a temperature controller (Model Ecoline RE-100, LAUDA, Germany). The size and zeta-potential of the nanoparticles were measured by a light-scattering machine equipped with an electrophoresis cell, ELS-800 (OTSUKA ELECTRONICS CO., LTD., Japan). A Millipore MILLEX AP 20 (nominal pore size of 500 nm) filter was used to remove dust from the samples for light-scattering measurements. TEM images were obtained by using a transmission electron microscope (H-500, Hitachi). A JEOL (Tokyo, Japan) ESR spectrometer was used to measure the X-Band ESR spectra. Cyclic voltammetry was performed with an electrochemical analyzer (ALS 600A). A glassy carbon (GC) working electrode was used in conjunction with a Pt counter electrode and a silver/silver chloride reference electrode.

Methods. The preparation of gold nanoparticles was carried out by mixing solutions containing MES or HEPES with an aqueous solution of 6 ppm Au(III). When necessary, the pHs of the buffer solutions were adjusted by the addition of a sodium hydroxide solution before the addition of Au(III). The same samples were used to measure the absorption spectra, size, zeta potential, and TEM image. The samples for TEM measurements were prepared by placing a drop of the colloid solution on a copper grid coated with a thin amorphous carbon film; any excess solution was removed by absorbent paper. The sample was then allowed to stand for a few hours for drying before being it placed in a specimen holder.

An aqueous solution of 0.1 mol dm^{-3} MES or HEPES was used for cyclic voltammetric measurements. Sodium sulfate of 0.20 mol dm^{-3} was maintained in these solutions as a supporting electrolyte. Before cyclic voltammetric (CV) measurements, the solution was flushed by argon gas for 5 min to remove dissolved oxygen. For ESR measurements, a solution containing 0.45 mol dm^{-3} of MES or HEPES was mixed with a solution of 30 ppm Au(III) just before the scan. The addition of a microgram-level of PBN was used as a spin-trapping agent for the MES sample.

Nanoparticle formation completed within a few minutes to about half an hour at 25 °C, depending on the experimental conditions, and the formed particles were stable over a period of weeks. The pH of the solutions was measured using a Beckman 32 pH meter. All experiments were conducted in a range of pH from 3.4 to 7.0. Moreover, 1.00×10^{-2} mol dm^{-3} sodium chloride was added in order to study the electrolyte effects on the generation of free radicals from the Good's Buffers as well as formation of gold nanoparticles. Under the present experimental conditions, the following Au(III) species predominantly exist, depending on the solution pH and chloride concentration: tetrachloroaurate ($[AuCl_4]^-$), trichlorohydroxoaurate ($[AuCl_3OH]^-$), dichlorodihydroxoaurate ($[AuCl_2(OH)_2]^-$), chlorotrihydroxoaurate ($[AuCl(OH)_3]^-$), and tetrahydroxoaurate ($[Au(OH)_4]^-$),[25,26] which react with the Good's Buffers to give nitrogen-centered radicals, resulting in the formation of gold nanoparticles. Therefore, free-radical generation as well as nanoparticle formation is independent of the Au(III) species. In other words, hydrolysis of the Au(III) species does not affect the generation of free radicals as well as the formation of nanoparticles. In addition, no ESR spectra were observed from the Good's Buffers in the presence of other metal ions, such as Mn(II), Fe(III), Co(II), Ni(II), Cu(II), Zn(II), Pd(II), Ag(I), Cd(II), Hg(II), or Pb(II).

The formation of gold nanoparticles by other Good's Buffers, such as EPPS, MOPS, MOPSO, HEPPSO, or PIPES, was also found. The gold nanoparticles formed from these Good's Buffers exhibited different colors (e.g., pink, pinkish, or bluish) and a range of absorption maxima (530 to 600 nm), depending on the Good's Buffers and their concentrations, pH and solutions' electrolyte concentration. Moreover, we have conducted the CV and ESR experiments for these Good's Buffers. All of these buffer reagents show a positive anodic peak (~+800 mV vs Ag/AgCl electrode) with different current intensities that are identical with MES or HEPES. Similar ESR spectra were also observed from these Good's Buffers in the presence of Au(III).

Results and Discussion

Characterization of Gold Nanoparticles. UV–Vis Absorption Spectra of Gold Nanoparticles: Figure 1 shows the UV–vis spectra of gold nanoparticles formed from MES solution at various experimental conditions: different concentrations of MES at pH 3.4–4.5 (a) and at pH 6.0 (b); the presence of 1.00×10^{-2} mol dm^{-3} sodium chloride for the corresponding pHs (c, d). Most of the spectra given in Fig. 1 show a single absorption peak (λ_{max}) in the visible range between 520 to 550 nm. Interestingly, there are two peaks in the UV–vis spectra for the nanoparticles formed at pH 3.4 of 0.10 mol dm^{-3} MES (Fig. 1a, spectrum 3, $\lambda_{max} = 530$ and 750 nm) and at the same solution, but containing 1.00×10^{-2} mol dm^{-3} NaCl (Fig. 1c, spectrum 3, $\lambda_{max} = 525$ and 822 nm). Moreover, spectrum 1 in Fig. 1d, corresponding to the nanoparticles formed at pH 6.0 of 1.00×10^{-3} mol dm^{-3} MES containing 1.00×10^{-2} mol dm^{-3} NaCl, shows a shoulder centered at 640 nm.

Similarly, the UV–vis spectra of gold nanoparticles formed from HEPES at pH 4.8–5.3 and pH 7.5 are shown in Figs. 2a and 2b, respectively. Very different from the gold nanoparticles formed from MES, which has a pinkish color, the colloids formed from HEPES are bluish to dark blue colors, depending on the HEPES concentration. This is also shown in Fig. 2 where a single broad absorption peak (λ_{max}) within the visible range between 550 to 580 nm can be observed. An exception is for spectrum 3 in Fig. 2a, standing for the nanoparticles formed from 0.10 mol dm^{-3} HEPES at pH 4.8, which appears at a higher wavelength (~650 nm), and even a broad peak. On the other hand, at a higher pH (pH = 7.5) the colloidal system becomes unstable for a HEPES concentration of 0.10 mol dm^{-3}, and the nanoparticles precipitate completely within a couple of hours, as indicated by the UV–vis spectrum (Fig. 2b, spectrum 3). Moreover, the addition of NaCl extremely destabilizes the colloids, and the nanoparticles precipitate within a few minutes. Hence, the UV–vis spectra of the gold nanoparticles formed from HEPES containing NaCl are not shown here.

It is known that spherical gold nanoparticles show a strong absorption band in the visible region between 520–550 nm. This absorption, called the plasmon resonance absorption,[27,28]

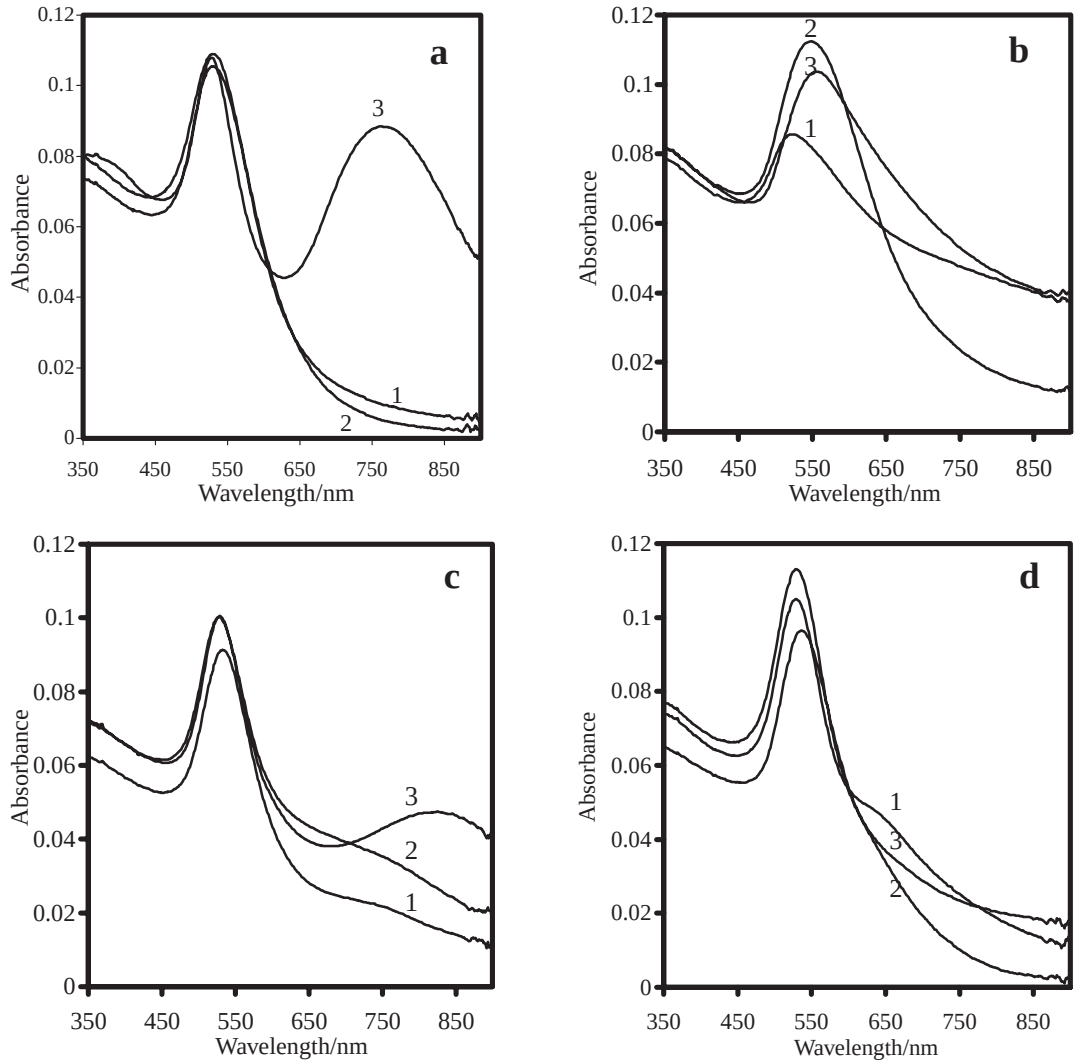

Fig. 1. UV–visible spectra of gold nanoparticles at various conditions of MES. Symbols a and b are for the solutions without pH adjustment and adjusted at pH 6.0 respectively and c and d are for the solutions without pH adjustment and adjusted at pH 6.0 with sodium chloride, respectively. The notations 1, 2, and 3 indicate the concentrations of MES of 1.00×10^{-3} (pH 4.48), 1.00×10^{-2} (pH 4.00), and 1.00×10^{-1} (pH 3.45) mol dm^{-3}, respectively. The gold and sodium chloride concentrations were maintained at 6 ppm and 1.00×10^{-2} mol dm^{-3}, respectively. The cell path-length is 10 mm.

is not observed for very small particles (2 nm and smaller) as well as for a bulk gold solution. It originates from the collective oscillation of the free electrons (6s-electrons of the conduction band in the case of gold) from the metallic atom. The plasmon absorption band depends on the size and shape as well as the aggregation behavior of the nanoparticles.[29–33] For nonspherical gold nanoparticles, however, the plasmon resonance splits into two modes: one longitudinal mode along the long axis of the non-spheroid and a transverse mode perpendicular to the first.[30] The longitudinal mode generally appears at a longer wavelength, depending on the aspect ratio; the transverse mode appears at a shorter wavelength (~530 nm). It is also known that the plasmon–plasmon interaction among the aggregated gold nanoparticles can produce an absorption band at ca. 650 nm,[29,31–33] which is, however, generally much broader than the plasmon resonance peak (ca. 525 nm). In many cases it appears as a shoulder,[31] rather than an isolated peak, depending on the degree and morphology of the aggregation.

The gold nanoparticles formed from an MES solution at a higher concentration (0.10 mol dm^{-3}), which have two absorption peaks (Fig. 1a, spectrum 3), are suggested to be a mixture of different shapes, e.g., spherical, hexagonal, pentagonal, octagonal or trigonal, etc., rather than due to random aggregations. These various geometrical shapes usually occur if the particle diameters are greater than 25 nm. In general, these alternations from the normal spherical shapes cannot be avoided, and reflect the crystalline nature of the colloidal particles.[34,35] On the other hand, the UV–vis spectra of gold nanoparticles formed from HEPES, especially at 0.10 mol dm^{-3} of HEPES, clearly indicate the aggregation behavior of these nanoparticles, which was also confirmed by TEM measurements. The intensive aggregation of gold nanoparticles formed from the HEPES, compared to those from MES, is ascribed to the higher pK_a value of HEPES (pK_a = 7.55) than that of MES (pK_a = 6.15).

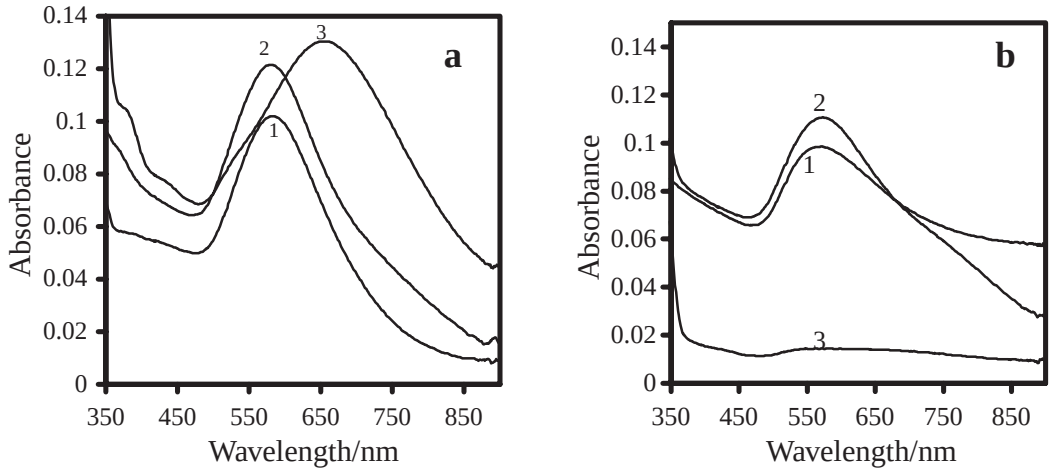

Fig. 2. UV–visible spectra of gold nanoparticles with different concentrations of HEPES. Here, a and b stand for the solutions without and with pH adjustment at 7.50, respectively. The notations 1, 2, and 3 indicate the concentrations of HEPES of 1.00×10^{-3} (pH 4.79), 1.00×10^{-2} (pH 5.17), and 1.00×10^{-1} (pH 5.27) mol dm^{-3}, respectively. The gold concentration was maintained at 6 ppm. The cell path-length is 10 mm.

Table 1. Sizes and Zeta Potentials of Gold Nanoparticles Observed by DLS and ELS with Different Concentrations of MES at Various pH and Sodium Chloride Concentrations

Concentration/mol dm^{-3}	pH	Size (*p.d.*[c])/nm		Zeta potential/mV	
MES		a	b	a	b
0.001	4.48	23 (0.30)	61 (0.31)	−29.86	−21.35
0.01	4.00	24 (0.32)	61 (0.33)	−29.64	−20.50
0.1	3.45	30 (0.35)	64 (0.35)	−28.15	−18.75
0.001	6.00	24 (0.31)	65 (0.33)	−26.56	−17.20
0.01	6.00	34 (0.31)	68 (0.34)	−18.42	−16.17
0.1	6.00	58 (0.33)	73 (0.35)	−14.92	−12.01

a) Without sodium chloride. b) With sodium chloride (1.00×10^{-2} mol dm^{-3}). The given values in the parentheses denote polydispersion coefficient. c) *p.d.* denotes the polydispersion coefficient of size distribution by DLS.

The electrolytes (NaCl) and pH affect not only the stability of the formed gold nanoparticles, but also the nanoparticle size, as discussed in the following section. The ionic strength effect is straightforward. It is known that the stability of nanoparticles depends on the ionic strength of the solution. The higher is the ionic strength, the greater is the aggregation of gold nanoparticles. The ionic-strength effect is accountable for an unstable colloidal system formed from 0.1 mol dm^{-3} HEPES at pH 7.5 (see Fig. 2b, spectrum 3). Since it is necessary to add NaOH to the HEPES solution for a pH adjustment (nearly 1:1 of NaOH and HEPES is required to obtain pH 7.5), the ionic strength of a solution of 0.1 mol dm^{-3} HEPES at pH 7.5 is much higher than those for spectra 1 and 2 in Fig. 2a.

Size and Zeta Potential of Gold Nanoparticles: Table 1 lists the size and zeta potential values for nanoparticles formed from MES under various conditions. The size does not change much with the concentration of MES at pH 3.4 to 4.5, with a typical size of 27 ± 3 nm and zeta values of −30 to −28 mV for different concentrations of MES. On the other hand, for samples formed from MES solutions at pH 6.0, a range of sizes (from 24 to 58 nm, increasing with the MES concentration) was observed, while the corresponding zeta potential values were reduced from −26.5 to −15.0 mV, respectively. Upon the addition of NaCl, larger sizes (approximately 60 to 70 nm) were generally observed compared to the corresponding samples containing no NaCl.

The effects of the pH and NaCl on the zeta potential are similarly explained. Under a higher ionic strength, it is presumed that the double layer of the gold nanoparticles is suppressed, resulting in a smaller zeta potential of the nanoparticles. Consequently, it is expected that the gold nanoparticles formed from 0.10 mol dm^{-3} MES at pH 6.0 containing NaCl should have the lowest zeta potential; this is the case, as listed in Table 1.

The size and zeta-potential values for the gold nanoparticles formed from HEPES under various conditions are given in Table 2. The apparent size was observed to be 35 ± 5 at pH 4.8 to 5.3 for different concentrations of HEPES, while the zeta-potential values were −28 to −24 mV. For samples prepared at pH 7.5, a range of size (32 to 40 nm) was observed for low concentrations of HEPES. However, at a high concentration (0.10 mol dm^{-3}) of HEPES, precipitation occurred and the corresponding zeta-potential values could not be determined.

Transmission Electron Micrography: Figures 3 and 4 illustrate typical electron micrographs of gold nanoparticles

Table 2. Size and Zeta Potential of Gold Nanoparticles Observed by DLS and ELS with Different Concentrations of HEPES at various pH

Concentrations /mol dm^{-3} HEPES	pH	Size (*p.d.*[b])/nm	Zeta potential/mV
0.001	4.79	30 (0.32)	−28.07
0.01	5.17	35 (0.32)	−26.26
0.1	5.27	40 (0.34)	−24.00
0.001	7.50	32 (0.33)	−26.67
0.01	7.50	40 (0.34)	−22.50
0.1	7.50	a)	a)

a) precipitated. The given values in the parentheses denote polydispersion coefficient. b) *p.d.* denotes the polydispersion coefficient of size distribution by DLS.

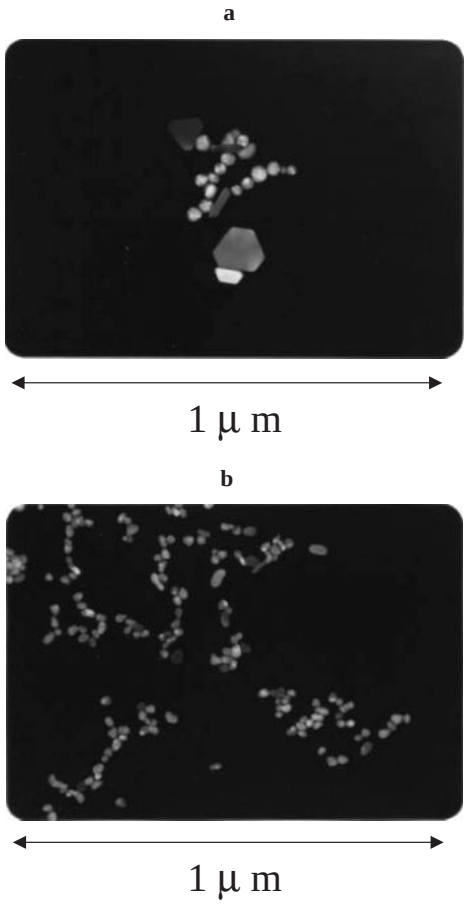

Fig. 3. TEM images of gold nanoparticles formed from MES. Symbols a and b are for 1.00×10^{-1} and 1.00×10^{-2} mol dm^{-3} of MES, respectively. Gold concentration was maintained at 6 ppm.

formed from MES and HEPES, respectively. Nanoparticles formed from 0.10 mol dm^{-3} MES at pH 3.5 show a mixture of differently shaped nanoparticles of finely dispersed, e.g., spherical, rod-like, hexagonal, pentagonal, or trigonal, etc., as shown in Fig. 3a. Different from spherical particles, nanoparticles of these geometric shapes generally have an aspect ratio (longitude to transverse axis) greater than unity, and are responsible for the splitting of the plasmon resonance absorption

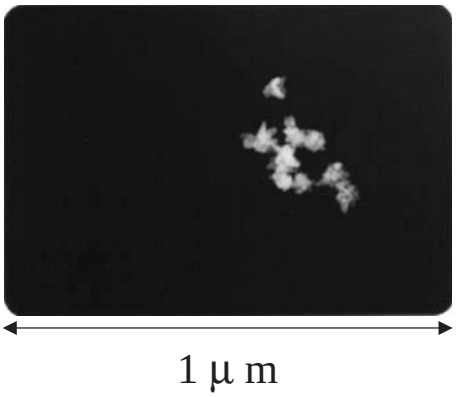

Fig. 4. TEM images of gold nanoparticles formed from 1.00×10^{-1} mol dm^{-3} of HEPES. Gold concentration was maintained at 6 ppm.

band, as depicted as spectrum 3 in Fig. 1a. The TEM images for HEPES indicate much more aggregation among the gold nanoparticles formed from the higher concentration (0.10 mol dm^{-3}) at pH 5.3, as can be seen in Fig. 4. In contrast, particles in Fig. 3b are seen to be more uniform and less agglomerated than those in Fig. 3a or Fig. 4. This finely dispersed nanoparticle (formed from 1.00×10^{-2} mol dm^{-3}, MES) nature is consistent with the UV–vis spectra, as shown in Fig. 1a (spectrum 2). Consequently, an identical size distribution of the gold nanoparticles formed from MES was observed in both DLS and TEM measurements (see Table 1 and Fig. 3). The aggregation behavior of gold nanoparticles formed from HEPES, observed by TEM, is also consistent with the UV–vis spectra of these samples. Obviously, the smaller nanoparticles formed from 0.10 mol dm^{-3} HEPES are not uniformly dispersed in the solution. Instead, extensive aggregation occurred, as shown in Fig. 4, resulting in intensive plasmon–plasmon interactions of the aggregated nanoparticles, which explains the very broad UV–vis absorption peak at longer wavelengths (spectrum 3 in Fig. 2a).

Formation Mechanism of Gold Nanoparticles. Electrochemistry: Figure 5 shows cyclic voltammograms of Good's Buffers, e.g., MES and HEPES. The voltammograms show only a single anodic peak at ~+800 mV vs Ag/AgCl, and no obvious cathodic peak could be observed. The development of positive anodic peaks from aqueous solutions of these buffer reagents clearly indicate that these buffering agents have mild reducing abilities. By contrast, gold(III) indicates a sharp cathodic peak (the forward scan, from positive to negative potential) with a hump, while the reverse scan indicates a low-intensity anodic peak, also with a hump, as shown in the inset of Fig. 5. The sharp cathodic peak is for the reduction of Au(III) to Au(II), while the hump is for Au(II) to Au(I).

Kinetics of the Formation of Gold Nanoparticles: The time-dependence absorption spectra of Au(III) in aqueous Good's Buffers indicate nanoparticles formation, which shows an induction period (~30 min), followed by a rapid formation of gold nanoparticles, as shown in Fig. 6. The results suggest a self-catalyzed reaction. The induction period depended on the experimental conditions.

Electron Spin Resonance Spectra: Figure 7 shows the ESR spectra of free radicals generated from an aqueous solu-

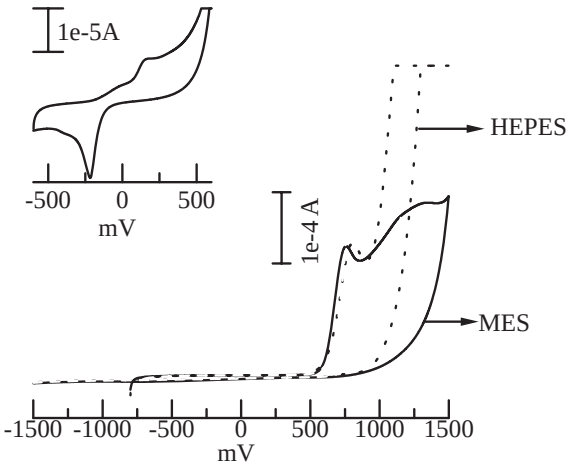

Fig. 5. Cyclic Voltammograms of Good's Buffers. A glassy carbon (GC) working electrode was used in conjunction with a Pt counter electrode and a silver/silver chloride reference electrode. Concentration of Good's Buffers was maintained at 0.10 mol dm^{-3}. The inset is the voltammogram for gold. Gold concentration was maintained at 30 ppm. 0.20 mol dm^{-3} of sodium sulfate was used a supporting electrolyte for both the experiments.

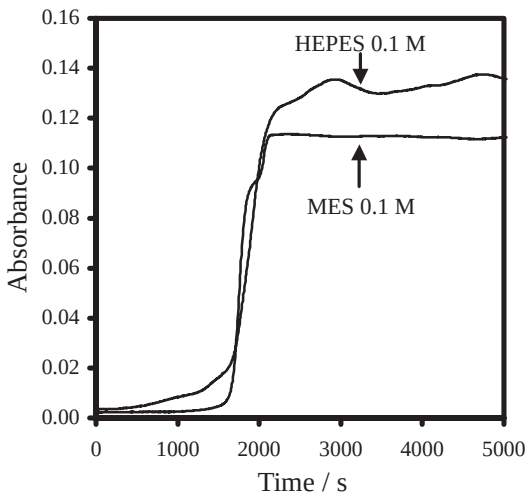

Fig. 6. Formation of gold nanoparticles by Good's Buffers as a function of time. Concentrations of Good's Buffers and gold concentration were maintained at 0.10 mol dm^{-3} and 6 ppm, respectively. The absorbance was at the absorption-maximum wavelength (λ_{max}) at 527 nm and 650 nm for MES and HEPES, respectively.

tion of MES and HEPES in the presence of gold(III). The ESR signals from the HEPES solution were readily observed. In contrast, there was no ESR signal from the MES solution until a micro-gram level of a free-radical trapping agent, PBN, was added to the solution. We were surprised not to observe the characteristic ESR signal from PBN in the case of MES, as one might expect. It is explained that the original MES radicals are extremely unstable, and PBN can take electrons from those highly labile MES radicals. It is, however, due to the much higher concentration of MES than PBN, that MES will again get electrons from PBN, and finally gives the ESR signals.

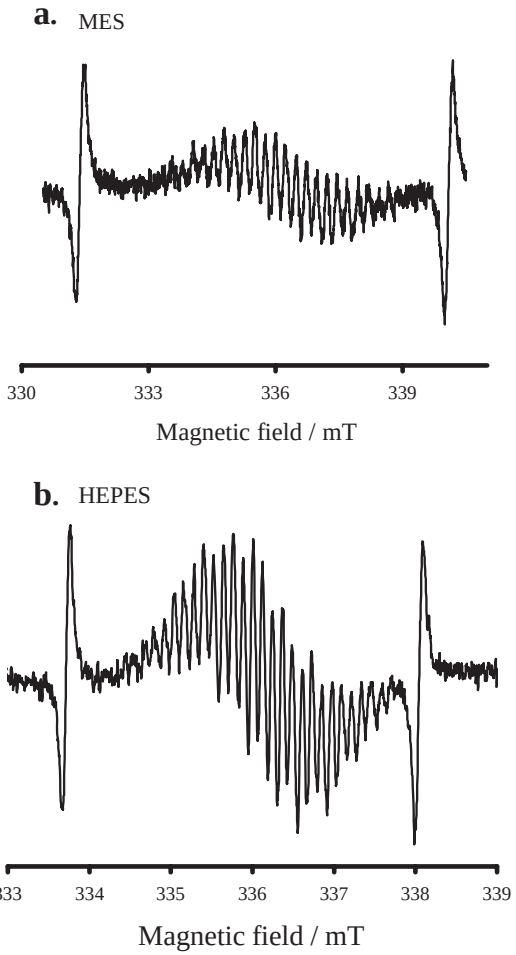

Fig. 7. ESR spectra of radicals produced from the oxidation of MES (a) of pH 3.4 and HEPES (b) of pH 4.4 in the presence of 30 ppm of Au(III). Conditions: 0.45 mol dm^{-3} buffers, room temperature, atmospheric pressure, and in the presence of a microgram amount of PBN for MES. Instrument settings: field set, 335 mT; sweep, 10 mT for MES and 20 mT for HEPES; scan rate, 4 min; modulation amplitude, 0.63 mT; gain 790; and power, 2.0 mW.

In other words, PBN may act as an intermediate that stabilizes the MES radicals. Moreover, the ESR signals of a small amount of PBN might be overlapped within the hyperfine ESR signals forest of MES.

The determined ESR parameters for MES and HEPES are almost identical: $g = 2.0074 \pm 0.0003$ and $a = 2.40 \pm 0.02$ G. These parameters are in agreement with those reported for HEPES in the presence of Fe(II), Fe(III)–polymer, and oxygen,[17] which suggest the formation of nitrogen-centered cationic free radicals.[17,18] Grady el al.[17] reported that Good's Buffers (HEPES and PIPES, etc.) having piperizine ring N-substituted with an alkyl sulfonate group is required for the formation radicals. It was found that the ESR spectra are generated from MES having a morpholine ring with an N-substituted alkyl sulphonate group in the presence of Au(III). The above results suggest that an alkyl sulphonate group attached to either an N-substituted piperazine ring or a morpholine ring also forms nitrogen-centered cationic free radicals in the presence of Au(III). Moreover, we also observed the same ESR

spectra from the Good's Buffers in the presence of Au(III) at different pH values (3.4, 4.0, 4.5, 5.0, 6.0, and 7.0) in the absence or presence of 1.00×10^{-2} mol dm^{-3} sodium chloride, where the Au(III) species are: $[AuCl_4]^-$, $[AuCl_3(OH)]^-$, $[AuCl_2(OH)_2]^-$ or $[AuCl(OH)_3]^-$.[25,26] Therefore, it is suggested that the formation of free radicals from the Good's Buffers is independent of the Au(III) species.

The cyclic voltammetric results indicated the mild reducing abilities of the Good's Buffers. Moreover, the generation of free radicals at different pH values and chloride concentrations from the Good's Buffers in the presence of Au(III), resulting in the formation gold nanoparticles suggested the following mechanism for the reactions between the buffer agents and the Au(III):

$$\text{Au(III)} + \text{Good's Buffers} \rightarrow \text{Au(II)} + \text{Cationic free radicals of Good's Buffers} \quad (1)$$

$$2\text{Au(II)} \rightarrow \text{Au(III)} + \text{Au(I)} \quad (2)$$

$$\text{Au(I)} + \text{Good's Buffers} \rightarrow \text{Au(0)} + \text{Cationic free radicals of Good's Buffers} \quad (3)$$

$$n\text{Au(0)} \rightarrow (\text{Au(0)})_n, \text{ gold nanoparticles} \quad (4)$$

$$\text{Cationic free radicals of Good's Buffers} + O_2 \rightarrow \text{Degraded products.} \quad (5)$$

Experiments aimed at identifying the degraded Good's Buffers reagents were also carried out. This was done by mixing a Au(III) solution with a given MES or HEPES solution. The formed nanoparticles were filtered and the pH of the solution were adjusted before a successive addition of the Au(III) solution. After several additions, it was found that no more gold nanoparticles could be formed from the MES or HEPES solution, although free Au(III) existed in the solution. The UV–vis spectrum of the MES or HEPES solution showed a distinctive absorption peak at approximately 346 nm, despite the fact that both MES and HEPES are transparent at this wavelength region, which suggests the formation of nitro-compounds as the degraded of MES or HEPES.

Conclusion

Good's Buffers are popular pH Buffers in chemistry, biochemistry, and biology laboratories, and also for tissue culturing purposes. It is interesting to find that these buffering reagents can easily reduce Au(III) to form gold nanoparticles in aqueous solutions at various pH values and ionic strengths. Our investigation revealed that the sizes of gold nanoparticles are sensitive not only to the concentration of the electrolyte, but also to the pH and types of Good's Buffers and their concentrations. Thus, different sizes of gold nanoparticles form under various conditions. The gold nanoparticle formation was not due to room light. Even being kept in the dark, gold nanoparticles were produced from $NaAuCl_4$ in the presence of Good's Buffers. On the other hand, no gold nanoparticles were formed in the absence of Good's Buffers from only gold aqueous solutions.

The cyclic voltammetry data indicated that these buffering compounds have a mild reducing ability. The ESR data indicate the formation of nitrogen-centered cationic radicals from the Good's Buffers in the presence of Au(III). The generation of identical ESR spectra at different pH values and chloride concentrations further suggested that the radical generation as well as nanoparticle formation is independent of the Au(III) species. Alternatively, hydrolysis did not affect the generation of radicals or the formation of gold nanoparticles. No ESR spectra were observed from the Good's Buffers in the presence of other metal ions, such as Mn(II), Fe(III), Co(II), Ni(II), Cu(II), Zn(II), Pd(II), Ag(I), Cd(II), Hg(II), or Pb(II). We, therefore, conclude that although an easy formation of gold nanoparticles in the presence of the Good's Buffers may be helpful to prepare of gold nanoparticles, these buffer reagents could be toxic in vitro studies where Au(III) is involved.

The authors thank Professor Sunao Yamada and the Center of Advanced Instrumental Analysis, Kyushu University for the measurement of TEM and Dr. Midori Yasuda, Nishi Kyushu University for the measurement of CV, and appreciate financial support in part by a PSJP scholarship (M.A. Habib) and Grants-in-Aid, B (No. 15350046) (M. Tabata), from the Ministry of Education, Culture, Sports, Science and Technology.

References

1 P. Alivisatos, *J. Phys. Chem.*, **100**, 13226 (1996).
2 E. Hutter, J. H. Fendler, and D. Roy, *J. Phys. Chem. B*, **105**, 11159 (2001).
3 M. J. Natan and L. A. Lyon, "Surface Plasmon Resonance Biosensing with Colloidal Au Amplification," 1st ed, ed by D. L. Feldhiem and C. A. Foss, Jr., Marcel Dekker, New York (2002), Vol. 1, pp. 183–205.
4 L. A. Lyon, M. D. Musick, and M. J. Natan, *Anal. Chem.*, **70**, 5177 (1998).
5 H. Q. Zhao, L. Lin, J. R. Li, J. A. Tang, M. X. Duan, and L. Jiang, *J. Nano. Res.*, **3**, 321 (2001).
6 M. Bendayan and S. Garzon, *J. Histochem. Cytochem.*, **36**, 597 (1988).
7 M. Bendayan, A. Nanci, and F. W. K. Kan, *J. Histochem. Cytochem.*, **35**, 983 (1987).
8 J. Wang, D. Xu, A. N. Kawde, and R. Polsky, *Anal. Chem.*, **73**, 5576 (2001).
9 M. Su, S. Li, and V. P. Dravid, *App. Phys. Lett.*, **82**, 3562 (2003).
10 S. J. Park, T. A. Taton, and C. A. Mirkint, *Science (Washington, D.C.)*, **95**, 1503 (2002).
11 Z. Ma, J. Li, L. Jiang, M. Yang, and S. F. Sui, *Chem. Lett.*, **2002**, 328.
12 H. Cai, Y. Wang, P. He, and Y. Fang, *Anal. Chim. Acta*, **469**, 165 (2002).
13 N. E. Good, G. D. Winget, W. Winter, T. N. Connolly, K. Izana, and R. M. M. Singh, *Biochemistry*, **5**, 467 (1966).
14 N. E. Good and K. Izawa, "Methods in Enzymology," Academic Press, New York (1972), Vol. 24, pp. 43–68.
15 A. Fisk and S. Pathak, *Nature (London)*, **224**, 1030 (1969).
16 T. F. Dyer and D. A. Cocks, *Ann. Clin. Biochem.*, **17**, 214 (1980).
17 J. K. Grady, N. D. Chasteen, and D. C. Harris, *Anal. Biochem.*, **173**, 111 (1988).
18 W. C. Danen and R. C. Rickard, *J. Am. Chem. Soc.*, **94**, 3254 (1972).
19 K. Hegetschweiler and P. Saltman, *Inorg. Chem.*, **25**, 107 (1986).

20 R. Nakon and C. R. Krishnamoorthy, *Science*, **221**, 749 (1983).
21 R. Nakon, *Anal. Biochem.*, **95**, 527 (1979).
22 J. M. Pope, P. R. Stevens, M. T. Angotti, and R. Nakon, *Anal. Biochem.*, **103**, 214 (1980).
23 E. A. Lance, C. W. Rhodes, III, and R. Nakon, *Anal. Biochem.*, **133**, 492 (1983).
24 E. Nyarko, T. Hara, D. J. Grab, A. Habib, Y. Kim, O. Nikolskaia, T. Fukuma, and M. Tabata, *Chemico-Biological Interact.*, **148**, 19 (2004).
25 A. Habib, M. Tabata, and Y. Wu, *J. Porphyrins Phthalocyanins*, in press.
26 C. F. Baes, Jr. and R. E. Mesmer, "The Hydrolysis of Cations," Krieger Publishing Company, Florida (1986), pp. 279–286.
27 M. Kerker, "The Scattering of Light and Other Electromagnetic Radiation," Academic Press, New York (1969).
28 F. Bohren and D. R. Huffman, "Absorption and Scattering of Light by Small Particles," John Wiley, New York (1983).
29 M. H. Rouillat, I. R. Antoine, E. Benichou, and P. F. Brevet, *Anal. Sci.*, **17**, i235 (2001).
30 S. Link, M. B. Mohamed, and M. A. El-Sayed, *J. Phys. Chem. B*, **103**, 3073 (1999).
31 S. L. Westcott, S. J. Oldenburg, T. R. Lee, and N. J. Halas, *Chem. Phys. Lett.*, **300**, 653 (1999).
32 U. Kreibig and M. Vollmer, "Optical Properties of Metal Clusters," Springer, New York (1995).
33 M. Quinten and U. Kreibig, *Surf. Sci.*, **172**, 557 (1986).
34 M. A. Hayat, "Colloidal Gold; Principles, Methods, and Applications," Academic Press (1989), Vol. 1, pp. 15–27.
35 S. L. Goodman, G. M. Hodges, L. K. Tredjdosiewicz, and D. C. Livingston, *J. Microsc.*, **123**, 201 (1981).